

Traps for simultaneous removal of SO_x and vanadium in FCC process

Luis Cedeño Caero^{a,b,*}, Luis C. Ordóñez^a, Jorge Ramírez^a, Francisco Pedraza^b

^a UNICAT, Facultad de Química, Universidad Nacional Autónoma de México, Cd. Universitaria, 04510 Mexico D.F., México

^b Instituto Mexicano del Petróleo, 07730 México D.F., México

Available online 16 August 2005

Abstract

Simultaneous removal of SO_x and vanadium under simulated fluid catalytic cracking (FCC) regenerator conditions was studied over mixed oxide traps of Ti–Al–Mg doped with La. These materials were prepared by the sol–gel method and characterized by DTA/DTG, X-ray diffraction (XRD), N₂ adsorption–desorption, SEM–EDX and UV–vis–DRS. The capacity of the traps was determined by means of a thermogravimetric study for SO_x removal and V capture hydrothermal tests followed by chemical analysis for vanadium trapping. The traps performance results under simulated FCC conditions show that these traps exhibit an excellent performance for SO_x removal with the presence of vanadium compounds, and high V capacity in presence of sulphated compounds.

© 2005 Elsevier B.V. All rights reserved.

Keywords: FCC; Mixed oxides; Lanthanum; SO_x removal; Ti–Al–Mg; Vanadium traps

1. Introduction

The catalytic performance of the ultra stable Y zeolite used as catalyst in the fluid catalytic cracking (FCC) process is seriously affected by metal contaminants, such as vanadium or nickel, presents in crude oil as organic complexes. These organic species, mostly porphyrins, are deposited on the catalytic surface and V oxide compounds are formed. Vanadium compounds promote undesirable dehydrogenation reactions, which increase coke production at the expense of gasoline yield [1]. Moreover, vanadium decreases the overall catalytic activity and selectivity by destroying the zeolite crystallinity. In the FCC reactor, the porphyrins containing vanadium in +3 or +4 oxidation states are decomposed and the reduced vanadium deposits onto the surface of the catalyst, along with coke. In the regenerator, coke burns off the catalyst and the vanadium oxidizes into the +4 and +5 state. Then, mobile vanadium species, such as vanadic acid, are formed by reaction of the oxidized vanadium with steam. Vanadic acid can move from particle to particle and can also migrate into the catalyst, accelerating the deactivation of fresh catalyst

particles. A method of protecting the catalysts from V deactivation is to use traps that prevent V from contacting with the catalyst [2]. One common type of V traps contains a basic species that reacts with and neutralizes acidic V compounds. Among the compounds that have been proposed as V traps are titania and magnesium oxides. These basic compounds theoretically react with vanadic acid and bind it in the trap.

Another important problem in the FCC process is the presence of pollutants, such as SO_x. During the coke burn-off in the FCC regenerator, sulfur oxides are converted into sulfate on the catalyst, which is subsequently released as H₂S in the reactor. This step rejuvenates the catalyst, which is then recirculated through the regenerator, and the cycle is repeated. Group IIA metals favor the capture of SO₃ and the formation of metal sulfate. In addition, Al₂O₃ has been disclosed as a potential oxide for the capture of SO₃. The materials most used in SO_x reduction are additives that contain MgO or rare-earth oxides supported on alumina [3,4]. Depending on the concentration and nature of the trap components, vanadium trap materials may or may not be affected by sulfur competition. In industrial applications, different traps are used specifically for SO_x or V removal. To tackle the problem of simultaneously removing SO_x and vanadium, we proposed in previous studies [5,6], the

* Corresponding author. Tel.: +52 55 56225366; fax: +52 55 56225366.
E-mail address: caero@servidor.unam.mx (L.C. Caero).

preparation of solids containing titania, alumina and magnesia. The results from this study showed that the synthesized materials present activity during several cycles but after continuous use some deterioration of the textural properties was observed, due to the phase transformation of titania–anatase to rutile. In order to improve the performance of these traps in this study, we modified the Ti–Al–Mg ternary oxides with La to increase their stability under FCC conditions, while maintaining high capacity for simultaneous SO_x and V removal. The choice of La was based on reports showing that La has better trapping capabilities than cerium [7], and La improves the SO_2 to SO_3 oxidation reaction, which is important in additives for SO_x control [8,9].

2. Experimental

2.1. Preparation of materials

Ti–Al–Mg ternary oxides synthesized as described in [5] were modified with 10 wt.% of La and will be referred as Ti_xLa , where x is the Ti molar percentage (10, 20 and 30%) in a $\text{Ti}(x)\text{--Al}(20)\text{--Mg}(80 - x)$ formulation with constant 20% mole of Al. Titanium (99%) and aluminum (98%) isopropoxides, magnesium metoxide (99.9%), absolute ethyl alcohol and nitric acid (3 M) were supplied by Aldrich. A mixture of Ti and Al precursors in alcoholic media was added to the Mg precursor, the alcohol/Al-precursor molar ratio was 60. The mixture was brought to reflux at 80 °C and stirred for 3 h. At room temperature, nitric acid was added with an acid/Al-precursor molar ratio of 0.03. Later as, lanthanum nitrate dissolved in deionized water was added drop-by-drop for polycondensation and aged during 24 h. The samples were dried at 100 °C for 3 days, and afterwards, these samples were calcined in static air at 650 °C for 4 h. Additionally, to evaluate the effect of the Mg precursor, Ti_{10}La and Ti_{30}La formulations were prepared using $\text{Mg}(\text{NO}_3)_2$ as Mg precursor, these samples will be referred as $\text{Ti}_{10}\text{NMgLa}$ and $\text{Ti}_{30}\text{NMgLa}$, respectively. Samples without La, Ti_{10} and Ti_{30} , were also prepared as references.

2.2. Characterization

Calcined materials were characterized by several techniques: X-ray diffraction (XRD) patterns were recorded using a Siemens D500 powder diffractometer with $\text{Cu K}\alpha$ radiation. Surface areas and N_2 adsorption–desorption isotherms were measured with an ASAP 2000 Micromeritics apparatus. Nitrogen physisorption isotherms were analyzed using the BET and BJH method. Prior to the textural characterization the samples were outgassed for 8 h in vacuum at 270 °C.

Elemental composition was evaluated by atomic absorption using a Perkin-Elmer spectrophotometer model S-2380, and also by SEM–EDX with a Stereoscan 440 Leica

microscope equipped with an energy dispersive X-ray (EDX)-elemental analysis system. UV–vis diffuse reflectance spectra were recorded with a Cary 5E UV–vis–NIR spectrometer.

TGA/DTA thermograms were obtained with 40 mg of uncalcined sample dried overnight at 100 °C. The samples were heated, under flow of air (40 mL/min), from RT to 1000 °C at heating rate of 20 °C/min. The thermograms of the fresh samples were recorded in a Perkin-Elmer TGA-2/DTA 1700, using calcined alumina as reference material.

2.3. V trap effectiveness

V capture hydrothermal test was carried out to evaluate the V trap effectiveness, in which the V impregnated catalyst is steam-treated to simulate aging of the metals and deactivation of the catalyst in similar conditions to the FCC unit [10]. An FCC catalyst impregnated with 3900 ppm of V using organometallic compounds [11], was mixed with the trap (80/20 wt.%). The mixture was steamed at 788 °C, for 10 h in a 100% steam environment at atmospheric pressure, as is described in [12]. The FCC catalyst and trap were separated by differences in density using a diiodomethane–acetone solution. The V contents in the FCC catalyst and the trap were evaluated by atomic absorption and SEM–EDX.

2.4. SO_x adsorption–reduction capacity

The SO_x adsorption–reduction capacity of the samples was evaluated gravimetrically using a TGA system according to [13]. SO_x pickup and H_2 reduction were studied. After pretreatment of 40 mg of trap in flowing N_2 at 600 °C for 1 h, the temperature was lowered to 520 °C. Subsequently, a stream of 100 mL/min with 0.76% SO_2 , 14.28% O_2 and 84.96% N_2 was introduced into the system. The maximum SO_x adsorbed was defined as the maximum amount of SO_x adsorbed per gram of trap, when the thermogram reaches the adsorption equilibrium. After the adsorption, the system was purged with N_2 at 550 °C and stabilized. Afterwards, a flow of 35% H_2/Ar (100 mL/min) was introduced for trap regeneration at 650 °C. Under these conditions, the SO_x adsorbed and reduction rates were evaluated from the TGA slope during the first 10-min for each cycle. This cycle was repeated several times to evaluate the effect of adding and removing sulfur to a potential SO_x catalyst in order to reveal a possible deactivation. To assess the effect of the presence of V on the SO_x sorption capacity, the V capture hydrothermal and SO_x pickup test were carried out successively.

3. Results and discussion

3.1. Traps characterization

The elemental composition of traps obtained by atomic absorption was similar to the theoretical composition used in

Table 1
Nominal composition and textural properties of the calcined samples

| Sample | Ti ^a (%) | Mg ^a (%) | Mg precursor | Area BET (m ² /g) | Pore diameter (Å) | Pore volume (cm ³ /g) |
|-----------------------|---------------------|---------------------|--------------|------------------------------|--------------------------|----------------------------------|
| Ti10 | 10 | 70 | Methoxide | 321 | 61 | 0.70 |
| Ti10La | 10 | 70 | Methoxide | 253 | 110 and 330 ^c | 0.80 |
| TvTi10La ^b | 10 | 70 | Methoxide | 65 | 150 and 290 ^c | 0.37 |
| Ti10NMgLa | 10 | 70 | Nitrate | 102 | 60 | 0.18 |
| Ti20La | 20 | 60 | Methoxide | 262 | 77 | 0.70 |
| Ti30 | 30 | 50 | Methoxide | 243 | 65 | 0.65 |
| Ti30La | 30 | 50 | Methoxide | 280 | 72 | 0.70 |
| Ti30NMgLa | 30 | 50 | Nitrate | 96 | 46 | 0.14 |

^a Theoretical mole percentage of metal, with constant 20% of Al.

^b TvTi10La is the Ti10La sample after V capture hydrothermal test.

^c Bimodal distribution.

the preparation. Theoretical composition and N₂ adsorption–desorption results from the synthesized materials and the La-free references, Ti10 and Ti30, are given in Table 1. Ti_xLa series has about 260 m²/g with a mean pore diameter of about 70 Å and a pore volume between 0.7 and 0.8 cm³/g. After the V capture hydrothermal test, the surface area and pore volume of the trap decreased significantly as can be observed in Table 1, for TvTi10La. Similar results were obtained from the other samples. However, these textural properties are adequate for SO_x traps in view of the drastic FCC operation conditions. After hydrothermal treatment, La-free traps showed poorer textural stability. For example, Ti10 presented 321 m²/g before and 31 m²/g after hydrothermal test. In contrast, the area of the La-containing trap (Ti10La) changed from 253 to 65 m²/g, before and after hydrothermal test, respectively. This indicates clearly the textural stabilization properties of La under FCC conditions.

The XRD pattern of the calcined samples showed only the formation of magnesium oxide in the periclase phase, which is obtained at about 460 °C according to TGA and DTA profiles (not shown). After the hydrothermal test (at 788 °C in steam flux), the samples present other phases, as MgTiO₃ and traces of LaVO₃. These results are presented in Table 2.

For the Ti_xLa sample obtained with Mg metoxide, the SEM micrographs showed small white spots, whereas the Ti_xNMgLa samples, obtained with Mg nitrate, exhibit a homogenous surface (see Fig. 1). Table 3 shows the average of EDX-elemental quantitative analysis results, obtained from several particles. The analysis of the small white spots revealed an increased concentration of La and V, and

therefore these spots can be associated to zones with a high concentration of La and V species. According to XRD analysis, we observed traces of LaVO₃ in these samples. EDX analysis of Ti_xNMgLa samples revealed a higher magnesium superficial content than Ti_xLa. In agreement with the higher magnesium surface concentration of samples Ti_xNMgLa, the UV–vis–DRS results (Fig. 2) indicated that these samples have a more pronounced insulating character than the Ti_xLa samples.

3.2. V capture hydrothermal tests

Myrstand et al. [14] studied the effect of the level of sulfur in FCC naphtha over the V capture capacity. The study shows that the capacity decreases with the sulfur content in the naphtha. For this reason, it is important to evaluate the effect of the SO_x presence on V capacities. Table 4 presents these results, which were obtained with and without SO_x during the hydrothermal test. These results corroborate the detrimental effect of the presence of SO_x over the V capture capacity. In the same table, the results of La-free samples are presented. For high contents of Ti ($x = 30$), the presence of La favors the V capture capacity whereas for low Ti contents ($x = 10$) less V is captured. However, these capacities are similar to those of commercial traps [6]. The V capacities for commercial traps were 25 and 30% of V removal, evaluated in similar conditions, but in the absence of sulfated compounds.

Table 3
Elemental analysis obtained by SEM–EDX of steamed samples, after V capture hydrothermal test

| Trap | Al (mole%) | Mg (mole%) | Ti (mole%) | La (wt.%) | V (ppm) |
|------------|------------|------------|------------|-----------|---------|
| Ti10La | 21.06 | 68.30 | 10.36 | 15.86 | 2402 |
| White spot | 24.45 | 66.30 | 9.25 | 32.33 | 2517 |
| Ti20La | 18.86 | 63.77 | 17.34 | 6.20 | 3282 |
| White spot | 24.83 | 57.73 | 17.43 | 21.16 | 5537 |
| Ti30La | 18.73 | 56.43 | 24.83 | 5.96 | 1218 |
| White spot | 23.01 | 53.21 | 23.78 | 22.04 | 3417 |
| Ti10NMgLa | 12.44 | 80.50 | 7.05 | 6.01 | 1355 |
| Ti30NMgLa | 14.80 | 63.71 | 21.48 | 6.46 | 2078 |

Table 2
XRD results of calcined and steamed (after V capture hydrothermal test) samples

| Sample | Calcined sample (at 650 °C for 4h) | Steamed sample (at 788 °C for 10 h) |
|-----------|------------------------------------|------------------------------------------------|
| Ti10La | MgO-periclase | MgO-periclase and MgTiO ₃ |
| Ti20La | amorphous | MgO-periclase and MgTiO ₃ |
| Ti30La | MgO-periclase | MgO-periclase and MgTiO ₃ |
| Ti10NMgLa | MgO-periclase | MgO-periclase and traces of MgTiO ₃ |
| Ti30NMgLa | MgO-periclase | MgO-periclase and MgTiO ₃ |

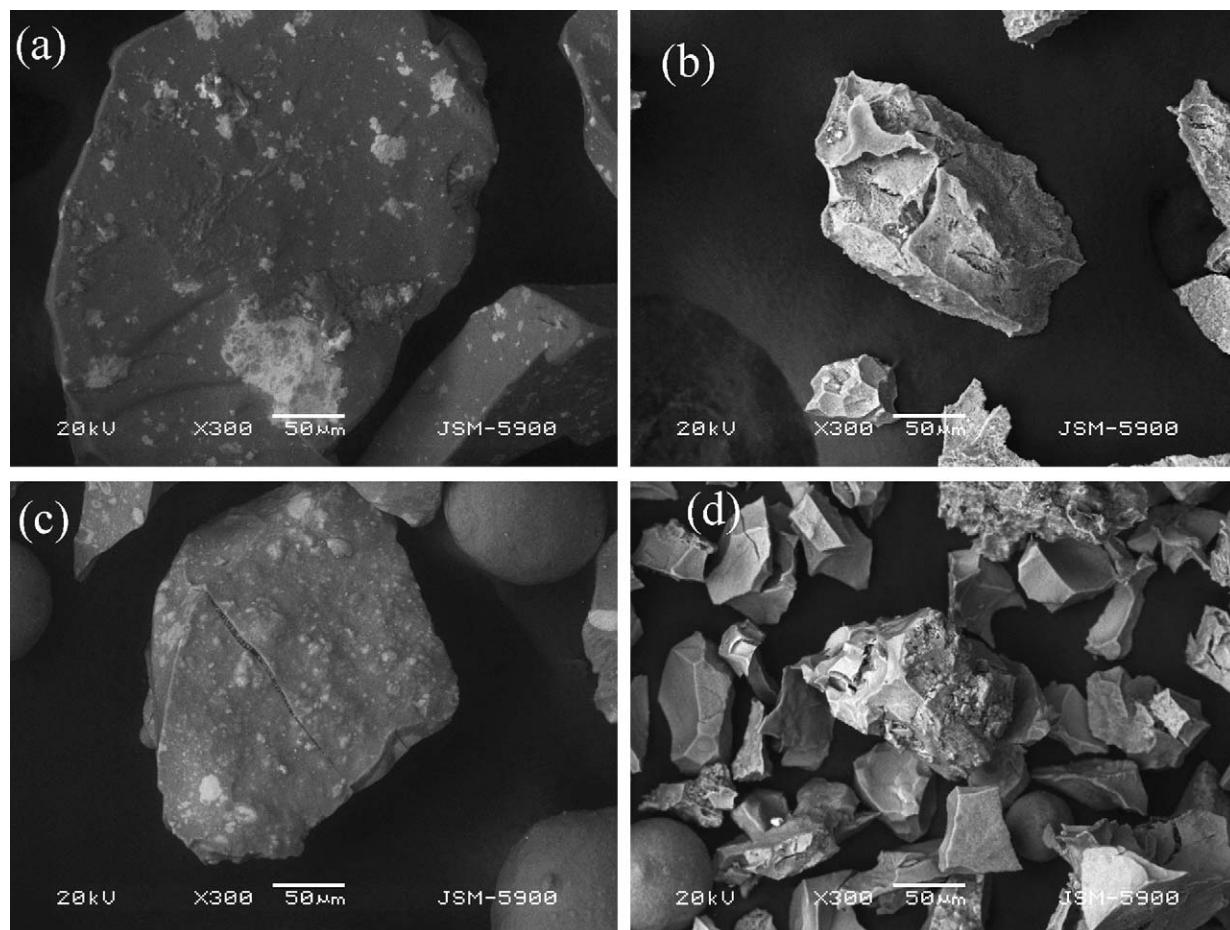


Fig. 1. SEM micrographs of: (a) Ti10La, (b) Ti10NMgLa, (c) Ti30La and (d) Ti30NMgLa.

The analysis of V content by EDX and atomic absorption (Tables 3 and 4) showed differences that can be rationalized on the basis of the principle of each technique. Whereas the atomic absorption analysis gives the bulk concentration, the EDX analysis probes only a depth ranging from 0.02 to

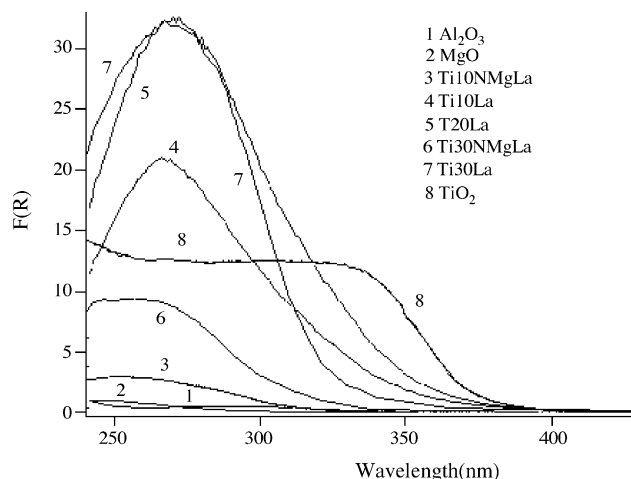


Fig. 2. Diffuse reflectance UV-vis spectra of the calcined samples.

several micrometers. Therefore, our results show a superficial enrichment of V, attributed to the presence of well-dispersed MgTiO_3 , as the XRD results suggested. The performance of MgTiO_3 for V trapping was evaluated in hydrothermal test showing, under similar conditions to the traps modified with La that this material is capable of capturing 10,200 ppm of V (equivalent to 65% of V captured), which is up to five times higher than the traps modified with La (see Table 3). Therefore, MgTiO_3 showed a high performance in V capture. It is possible then, that the increased capacity observed for the Ti_xLa traps is due to the presence of MgTiO_3 .

3.3. SO_x pickup tests

Tables 5 and 6 show adsorption–reduction SO_x results for two simulated reaction–regeneration FCC cycles, for samples without and with vanadium, respectively. Because the presence of MgTiO_3 was detected by XRD and also suggested by the SEM–EDX, the SO_x pickup capacity of pure MgTiO_3 was also tested to evaluate its contribution to this process; the results are presented in Table 5. MgTiO_3 showed the highest SO_x -adsorption rate, but the SO_x -desorption rate is slow compared to all other traps.

Table 4

V captured capacity for the traps obtained by atomic absorption, before and after SO_x pickup tests

| Traps | V captured ^a without SO _x | | V captured ^a with SO _x | | V captured ^a without SO _x (traps without La) | |
|-----------|-------------------------------------------------|------|----------------------------------------------|------|--------------------------------------------------------------------|------|
| | wt. % | ppm | wt. % | ppm | wt. % | ppm |
| Ti10La | 39.75 | 1550 | n.d. | n.d. | 50.64 | 1975 |
| Ti20La | 46.15 | 1800 | 24.36 | 950 | n.d. | n.d. |
| Ti30La | 42.18 | 1645 | 27.56 | 1075 | 33.33 | 1300 |
| Ti10NMgLa | 42.95 | 1675 | 28.85 | 1125 | 50.64 | 1975 |
| Ti30NMgLa | 48.72 | 1900 | 30.13 | 1175 | 33.33 | 1300 |

^a V captured represents the percentage of V removal from the FCC catalyst.

Table 5

SO_x adsorption–reduction results of calcined samples, before V capture hydrothermal test

| Sample | Maximum SO _x adsorbed (mmole/g) | | SO _x adsorbed rate (μmole/g min) | | SO _x reduction rate (μmole/g min) | |
|--------------------|--------------------------------------------|---------|---------------------------------------------|---------|----------------------------------------------|---------|
| | Cycle 1 | Cycle 2 | Cycle 1 | Cycle 2 | Cycle 1 | Cycle 2 |
| Ti10 | 7.2 | 5.7 | 37.6 | 53.1 | 81.6 | 52.1 |
| Ti10La | 4.7 | 4.3 | 35.0 | 47.0 | 6.2 | 5.9 |
| Ti20La | 11.0 | 15.2 | 66.9 | 133.1 | 69.4 | 97.5 |
| Ti30La | 10.6 | 11.2 | 63.5 | 94.8 | 115.5 | 112.4 |
| Ti30 | 7.9 | 5.9 | 63.9 | 56.6 | 84.2 | 66.5 |
| Ti10NMgLa | 6.8 | 9.8 | 37.5 | 67.8 | 119.2 | 141.3 |
| Ti30NMgLa | 4.4 | 5.0 | 38.7 | 69.7 | 126.4 | 143.5 |
| MgTiO ₃ | 4.5 | 5.6 | 100.6 | 74.0 | 10.3 | n.d. |

3.3.1. Adsorption–reduction activity of the traps in the absence of vanadium

In the samples without La (Ti_x), an increase in the relative concentration of Ti caused no significant change in the SO_x adsorption–desorption capacity. However, when La is incorporated, the activity depended on the Mg precursor. For samples prepared with Mg nitrate (Ti_xNMgLa) the activity increased with the Ti content, whereas for samples prepared with Mg metoxide (Ti_xLa) the activity decreased. The effect of the Mg precursor depended on the Ti content. For low Ti content ($x = 10$), the activity increased by changing from Mg metoxide to Mg nitrate. In contrast, for high Ti contents ($x = 30$), the reverse trend was observed.

MgTiO₃ shows important activity for SO_x adsorption–desorption. This compound would be formed at high Ti concentration. However, the XRD results in Table 2 and those in [5] show that MgTiO₃ is only present in the traps

modified with La. It appears then that the incorporation of La to the samples favors the formation of MgTiO₃ in the Ti-rich samples and, as Table 5 shows, La will increase the SO_x pickup capacity. Accordingly, the activity only increased significantly in La-containing traps with high Ti content.

3.3.2. Adsorption–reduction activity of the traps in the presence of vanadium

In presence of V (Table 6), similar behavior is observed in the different samples, although the activity values are smaller than for the V-free experiments. In general, the use of Mg metoxide and La incorporation favors the SO_x adsorption–reduction capacity.

The results of the second SO_x adsorption–reduction cycle in the presence and absence of V (Tables 5 and 6) indicate that the materials are stable. In fact, in some cases the

Table 6

SO_x adsorption–reduction results of steamed samples, after V capture hydrothermal test

| Sample | Maximum SO _x adsorbed (mmole/g) | | SO _x adsorbed rate (μmole/g min) | | SO _x reduction rate (μmole/g min) | |
|-----------|--------------------------------------------|---------|---------------------------------------------|---------|----------------------------------------------|---------|
| | Cycle 1 | Cycle 2 | Cycle 1 | Cycle 2 | Cycle 1 | Cycle 2 |
| Ti10 | 3.3 | 4.0 | 20.3 | 31.2 | 19.1 | 25.6 |
| Ti10La | 4.9 | 5.4 | 28.6 | 45.9 | 10.0 | 8.3 |
| Ti10NMgLa | 4.1 | 4.6 | 27.9 | 54.1 | 5.3 | 7.9 |
| Ti20La | 4.0 | 4.4 | 17.1 | 31.6 | 12.1 | 11.8 |
| Ti30 | 2.7 | 3.3 | 18.8 | 29.5 | 34.2 | 45.6 |
| Ti30La | 3.8 | 3.5 | 22.2 | 34.9 | 4.4 | 4.0 |
| Ti30NMgLa | 2.2 | 2.4 | 23.6 | 36.6 | 3.3 | 5.0 |

activity observed for the second cycle was better, especially in the presence of V.

No direct relationship was found between textural properties of the materials used here and the activity trends observed. However, the Mg content in the trap is an important parameter related to the activity of the trap.

The traps synthesized here exhibit high and stable performance for SO_x adsorption–reduction in the presence of vanadium compounds. They also exhibit high V removal capacity in the presence of sulfated compounds when compared to commercial traps. All of the above results appear to indicate that the enhanced V capture and SO_x pick up capacities are related to the presence of MgTiO_3 , which is favored at high Ti concentration for the traps modified with La. Therefore, these materials may be used as simultaneous V traps and SO_x reducer in FCC process.

4. Conclusions

Ti–Al–Mg mixed oxide traps doped with La was prepared by sol–gel method. These materials presented adequate textural properties before and after the V capture hydrothermal tests because of the presence of La. The incorporation of La was also beneficial to the SO_x adsorption–reduction capacity of the trap, especially in the presence of V.

The choice of the Mg precursor was important factor to the traps activity. When Mg nitrate was used a homogeneous surface was observed and Mg metoxide favored the SO_x adsorption–reduction capacity even in the presence of vanadium.

Ti–Al–Mg mixed oxides containing La displayed high activity for the simultaneous SO_x reduction in the presence

of vanadium and V-trapping performance in the presence of SO_x . Therefore, these materials may be used as simultaneous V traps and SO_x reducers in FCC process.

Acknowledgements

The authors are grateful to I. Puente for the SEM, R. Cuevas for the DTG/DTA work and IMP for the financial support through the FIES 98-23-III project.

References

- [1] G. Catana, W. Grunert, P. Van der Voort, E.F. Vansant, R.A. Schoonheydt, B.M. Weckhuysen, *J. Phys. Chem. B* 104 (2000) 9195.
- [2] T. Dougan, U. Alkemade, B. Lakhanpal, L. Boock, *Tech. Gas Oil J.* 26 (September) (1994) 81.
- [3] J. Yoo, A. Battacharyya, C. Radlowski, *Ind. Eng. Chem. Res.* 30 (1991) 1444.
- [4] B. Wen, M. He, C. Costello, *Energy Fuels* 16 (2002) 1048.
- [5] L. Cedeño, L. Ordoñez, F. Hernandez, F. Pedraza, *Emerging Fields in Sol–gel Science and Technology Materials*, vol. 1, Kluwer Academic Publisher, 2003, p. 230.
- [6] L. Cedeño, L. Ordoñez, F. Pedraza, *Información Tecnológica* 14 (4) (2003) 51.
- [7] K. Chao, L. Lin, Y. Ling, J. Hwang, L. Hou, *Appl. Catal. A* 121 (1995) 217.
- [8] V. Dimitriadis, I. Vasalos, *Ind. Eng. Chem. Res.* 31 (1992) 2741.
- [9] W. Cheng, G. Kim, A. Peters, X. Zhao, K. Rajagopalan, *Catal. Rev. Sci. Eng.* 40 (1998) 39.
- [10] B. Speronello, W. Reagan, *Tech. Gas Oil J.* 30 (January) (1984) 139.
- [11] B.R. Mitchell, *Ind. Eng. Chem. Prod. Res. Dev.* 19 (1980) 209.
- [12] ASTM D4463-96, reapproved, 2001.
- [13] A. Battacharyya, G. Woltermann, J. Yoo, J. Karch, W. Cormier, *Ind. Eng. Chem. Res.* 27 (1988) 1356.
- [14] T. Myrstad, B. Seljestokken, E. Rytter, *Appl. Catal. A* 192 (2000) 299.